Finite-Difference Time-Domain Modeling of Light-Trapping in Solar Cells

Todd Marshall and Melinda Piket-May
University of Colorado at Boulder
Campus Box 425
Boulder, CO 80309-0425
Fax: 303-492-2758 Email: mjp@boulder.colorado.edu

Abstract—**To maximize light-trapping, the absorption of light in the solar cell is maximized. The ways to increase light-trapping are to texture the surfaces of the solar cell and to use anti-reflection coatings. The power spectrum of sunlight also plays an important role in light-trapping. In general, a solar cell consists of multiple layers of dielectric materials. Each dielectric has a complicated surface texture geometry to increase light-trapping. This paper concentrates on solving Maxwell's equations for the general solar cell configuration under illumination from the sun. The absorption and maximum achievable current density are calculated and used to quantify light-trapping in a given solar cell design.**

Thin solar cells promise to yield higher current collection than thick solar cells at a lower cost [1]. Low cost solar cells are usually characterized by short diffusion length semiconductors. Most minority carriers created within the distance equal to the diffusion length contribute to the electrical current of a solar cell. Hence, the solar cell must be thin when low quality materials are used. As solar cells decrease in size, the ray-trace model becomes inaccurate as previously demonstrated in [2]. A full-wave Finite-Difference Time-Domain (FDTD) light-trapping model is demonstrated to accurately study light-trapping of thin-film solar cells.

I. Introduction

Solar cells are semiconductor devices designed to convert light into electrical power. In order to be cost effective they must be as efficient as possible. Solar cell efficiency is related to the percent of the incident sunlight converted into electrical power. One goal in the design of solar cell devices is to trap and absorb as much light as possible inside the semiconductor. In the language of the solar cell community, the goal is to maximize light-trapping.

One effective way to maximize light-trapping is to coat the semiconductor with a thin film which reduces reflection. This anti-reflective coating ensures a higher percentage of light enters the cell so more light is absorbed. A second effective approach to increase light-trapping is to texture the surface of the solar cell [1], [3], [4], [5], [6], [7], [8], [9]. The texture creates multiple reflections which will lead to increased light-trapping. The specific design of the textures is critical to maximize light-trapping. All commercial solar cell designs include encapsulation to protect the solar cell from nature. The effect of encapsulation on light-trapping is not well understood. The integration of the anti-reflection coating, encapsulation, and texture into the solar cell design determines the overall light-trapping capacity of a solar cell [10].

Historically, the solar cell industry did not have a means to effectively and accurately predict the light-trapping of a given solar cell geometry. Each solar cell was manufactured and then its efficiency was measured. This is expensive and time consuming. This research fills the need of the solar cell community by quantifying and predicting the light-trapping of a given solar cell design with the aid of numerical models. The result of this research provides industry a means to quantify the light-trapping capability of many different three-dimensional solar cell designs. By modeling light-trapping, the expensive and time consuming step of fabrication is streamlined. Only the promising designs need to be fabricated and tested. This, in turn, frees valuable resources which can be utilized to design more efficient solar cells. The basics of numerical solar cell analysis and the results of the ray-trace analysis were detailed in a companion paper [11]. A reader not familiar with solar cell analysis is encouraged to read the cited paper first.

II. Background

A full-wave model of light-trapping based on the finite-difference time-domain method (FDTD) method is designed to include three-dimensional surface textures, encapsulation, anti-reflection coatings, the energy spectrum of sunlight and the polarization of light. Unlike the ray-trace model, the FDTD model explicitly includes the wave properties of light. The FDTD model accounts for diffraction

due to small surface textures. Small geometric features are common on thin solar cells designed to optimize light-trapping.

This research uses the basic FDTD algorithm first developed by Kane Yee in 1966 to numerically solve Maxwell's Equations and then extended by Taflove. It has been extensively documented so the basic methodology will not be repeated here [12], [13], [14]. The general solar cell geometry with surface texture, encapsulation, and anti-reflection coating is described based on the requirements of the FDTD algorithm. A periodic boundary is introduced to reduce the required computer resources. Sunlight is incorporated into the FDTD model as an electromagnetic source. Finally, the light-trapping model is completed with an explanation of the measurement of light-trapping. The paper concludes with a general discussion concerning the limitations and capabilities of FDTD modeling for solar cells.

A. Optical Properties of Matter

The governing equations of light-trapping are Maxwell's equations

$$\frac{\partial \vec{E}}{\partial t} = \frac{1}{\epsilon}\nabla \times \vec{H} - \frac{\sigma}{\epsilon}\vec{E} \tag{1}$$

$$\frac{\partial \vec{H}}{\partial t} = -\frac{1}{\mu}\nabla \times \vec{E} \tag{2}$$

where both the electric field and magnetic field ($\vec{E}$ and $\vec{H}$) describe the interaction between light and the solar cell. The solar cell is described by its permittivity, ϵ, and permeability, μ.

The parameters, $\epsilon = \epsilon_r\epsilon_0$ and σ, describe the optical properties of the solar cell. These properties are quantified directly or through the optical parameters of refractive index, n, and the extinction coefficient, k. The quantities are related by

$$\epsilon_r = n^2 - k^2 \tag{3}$$

$$\sigma = 2nk\epsilon_0\omega \tag{4}$$

where c is the speed of light, ω is the angular frequency of light and ϵ_0 is the permittivity of free space [15].

In actual practice, the light illuminating a solar cell experiences dispersion. Specifically, the index of refraction depends on the wavelength of the incident light. The extinction coefficient also depends on wavelength and determines the amount of light that is absorbed in the solar cell [16]. The index of refraction varies over a wide range from 3.4 to 5.6 which means dispersion effects are important. The extinction coefficient varies by orders of magnitude. The extinction coefficient becomes small as wavelength increases which means little light is absorbed at the higher wavelengths. The higher wavelengths corresponds to lower energy photons. Solar cell designs must accommodate dispersion to ensure accurate light-trapping predictions. Solar cell designs must also overcome the small extinction coefficient by maximizing light-trapping.

B. Solar Cell Geometry

Defining the solar cell, or any object, in the FDTD model requires that coefficients be calculated at each field location in the FDTD grid based on the material properties. The coefficients are calculated based on the material parameters of permittivity, permeability, and conductivity. Yee's algorithm imposes a Cartesian grid on the solar cell and surrounding space. Consequently, the location of a field relative to the Yee grid and the material determines the values of the coefficients.

Similar to the ray-trace model, the FDTD model defines the solar cell as a set of materials and interfaces. Each surface separates different materials within the solar cell. The surface normal is not explicitly required by the FDTD model. Unlike the ray-trace model, the solar cell is not restricted to using three-node planar elements. The interfaces are defined as surfaces represented by an arbitrary function of x- and y-coordinates, $K(x, y)$as shown in Figure 1. The surface is confined to the rectangle between $Nx1 <= i <= Nx2$ and $Ny1 <= j <= Ny2$. For each field component, the corresponding material parameter is defined. This definition is generalized to multiple surfaces by defining N interfaces; $K1, K2, K3 \ldots KN$ as necessary.

The encapsulation layer and anti-reflection coatings are incorporated into the FDTD model by defining the necessary number of surfaces. One benefit of using surfaces to define the solar cell is the simplicity of defining a anti-reflection coating with as many layers as needed. In contrast, the ray-trace model only incorporated a two-layer anti-reflection coating while the FDTD model is unlimited. There is no difference between defining the solar cell and the anti-reflection coating, or even the encapsulation layers.

C. Periodic Boundary Condition

Scanning Electron Microscope pictures of chemically etched textured solar cells show a periodic structure [1]. This allows us to model the textured

solar cell as an infinite grid. The infinite grid allows us to use a periodic boundary condition which conserves valuable computer resources. In the ray-trace model, the periodic boundary is simple to implement by checking when a light ray hits a periodic boundary. On the contrary, the incorporation of the periodic boundary into the FDTD algorithm is complicated by the light interacting with the entire periodic boundary simultaneously. The light is not localized to a single thin ray at a single point on the periodic boundary. Instead, the light interacts along the entire periodic boundary. The FDTD algorithm models the entire light wave. As a result, the periodic boundary contends with the spatial distribution of power which is inherent to light traveling in various directions.

Since the FDTD algorithm calculates the values of field components, the periodic boundary is defined relative to field locations in the Yee grid. Figure 1 shows the periodic boundary and the Yee field locations at two different heights within the solar cell. The views show two slices of the solar cell which are perpendicular to the periodic boundary. The first view shows a planar slice at a height of k to coincide with the fields in the bottom half of Yee's unit cell. The x- and y-components of the electric field and the z-component of the magnetic field are contained in the transverse electric plane (TE-plane). Note, the TE-plane has no relation to TE modes in a waveguide. The TE-plane is defined because the electric field components lie in the plane and are transverse to the normal $\hat{z}$ direction. The field components are drawn as small arrows for the x- and y-components of the electric field and as a small circle for the magnetic field. The periodic boundary surrounds the silicon and is confined on the electric fields which are bounded by the rectangle; $Nx1 <= i <= Nx2 + 1$ and $Ny1 <= j <= Ny2 + 1$. The Transverse Magnetic plane (TM-plane) is shown in the second planar slice. The TM plane is a slice through the solar cell at a height of $k+1/2$ to coincide with the upper half of a Yee unit cell. The TM-plane contains the x- and y-components of the magnetic field and the z-component of the electric field. Again, the field components are drawn as small arrows for the x- and y-components of the magnetic field and as a small circle for the electric field. By alternatively stacking TM- and TE-planes one on top of the other, any FDTD model of the solar cell is defined. It is sufficient to incorporate the periodic boundary into both TM- and TE-planes separately and then apply the corresponding boundary condition to every planar stack in the entire FDTD grid.

Each field component in the Yee grid only depends on its nearest neighbors. For example, when calculating $E_x(i,j,k)$, the nearest surrounding fields used by the update equation are $H_z(i,j,k)$, $H_z(i,j-1,k)$, $H_y(i,j,k)$, and $H_y(i,j,k-1)$. The nearest neighbors can be found graphically by drawing the smallest contour path perpendicular to the field to be updated [13]. This graphical interpretation of Yee's equations is true for all component fields in the Yee grid. By drawing contours, the fields whose contours do not overlap the periodic boundary are known to be unaffected by the periodic boundary. However, the fields whose contours overlap the periodic boundary are affected by the periodic boundary. The fields that are unaffected by the periodic boundary are colored light grey in Figure 1. While the field components colored dark black in Figure 1 are affected by the periodic boundary. The dark black fields correspond to Yee update equations that need to be modified to incorporate the periodic boundary. As an example, the E_x field along the boundary, $j = Ny1$, uses the surrounding fields; $H_z(i,j,k)$, $H_z(i,j-1,k)$, $H_y(i,j,k)$, and $H_y(i,j,k-1)$. The $H_z(i,j-1,k)$ is not the "correct" field to use because of the periodic boundary. Instead, the field to use is $H_z(i,Ny2,k)$ which comes from "wrapping" the solar cell around the boundary. The field outside of the boundary is replaced by a field inside the geometrically opposing boundary. In general, the periodic boundary is incorporated into the FDTD algorithm by "wrapping" the inner fields on the opposing boundary onto the outer fields on the periodic boundary.

D. Light Source

Sunlight is incorporated into the FDTD model based on the standard total-field/scattered-field formulation (TFSF) of a light source [13]. The standard TFSF defines a closed surface. Inside the closed surface, an arbitrary plane wave is excited by adding source fields on the closed surface. The magnitude of the source fields determines the intensity of the light. The direction of the source fields determine the polarization of the incident light. Outside the surface, the source fields are removed so only scattered waves exist outside of the TFSF surface.

The standard TFSF does not include the periodic boundary. The periodic boundary removes the need for a closed TFSF surface which makes the light source trivial to implement in the FDTD model. Instead of a closed surface, a single plane is used. The TFSF plane is placed above the solar cell with a

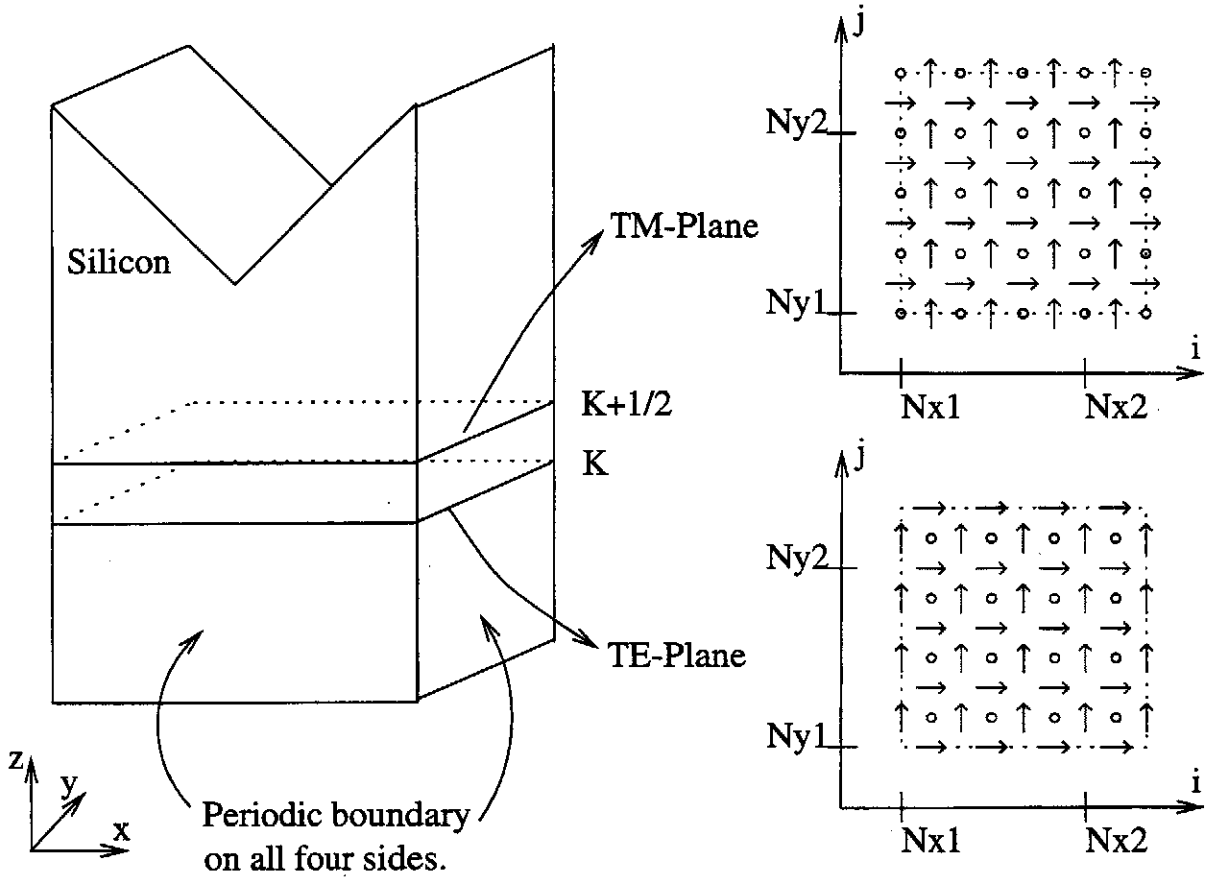

Fig. 1. The periodic boundary in the FDTD algorithm.

constant surface normal in the $\hat{z}$ direction as shown in Figure 2. Electric and magnetic fields are excited on the TFSF plane which excite the propagation of sunlight in the model. The periodic boundary ensures that the wave propagates correctly. Light only propagates in the $\pm\hat{z}$ direction, parallel to the periodic boundary.

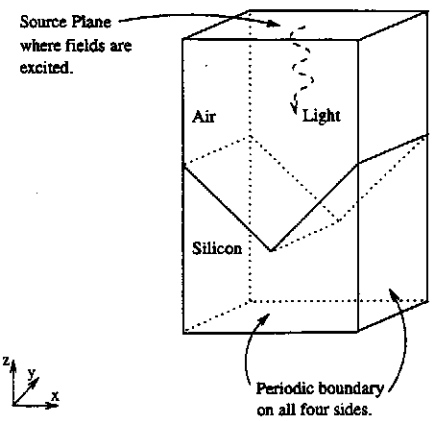

Fig. 2. The light source in the FDTD model with a periodic boundary.

E. Radiation Boundary Condition

As is the case with the ray-trace model, light which escapes from the solar cell causes numerical errors unless an effective radiation boundary condition is implemented. Unlike the ray-trace model, the radiation or absorbing boundary is difficult to implement into the FDTD model. There are many different solutions to the RBC but they all have inherent limitations [17], [18], [19], [20], [21], [22]. None of the various RBC's perfectly absorb all of the light. Some fraction of the light is always reflected back into the model. The Berenger Perfectly Matched Layer (PML) is the best algorithm for reducing the reflection error [23], [24]. To incorporate the PML into the light-trapping model, the PML is modified to include the periodic boundary. The periodic boundary in the PML is broken into two

steps, just like the normal Yee periodic boundary. First, the PML update is calculated. Second, the fields are wrapped around the periodic boundary.

F. Measurement of Light-Trapping

Absorption is the measure of light-trapping. The index of refraction and extinction coefficient vary as a function of frequency via the relation $\lambda\omega = 2\pi c$. The frequency dependent material properties of the solar cell dictate that a general method to calculate absorption is required by the light-trapping model. The FDTD model assumes a plane wave source with a general amplitude modulation to represent light. A common source modulation used is a Gaussian modulated sinusoid because it has a wide spectral content, is smooth, and is finite in duration. The finite duration allows actual computation run times to be reduced over a single sinusoid modulation. Also, the FDTD algorithm is not compatible with sources that are not smooth. The calculation of $A(\omega)$ is complicated by the frequency dependent solar cell materials and the general input source modulation requirement.

Absorption is the time averaged fraction of power absorbed to power incident which is given by

$$A = \frac{\langle P_{absorbed} \rangle}{\langle P_{source} \rangle} \tag{5}$$

and the time average power is

$$\langle P \rangle = \frac{1}{T} \int_{-T/2}^{T/2} P(t)\, dt \tag{6}$$

The total power absorbed within the solar cell volume, V, is

$$P_{absorbed}(t) = \sigma \int_V \vec{E}(\vec{r},t) \cdot \vec{E}(\vec{r},t)\, dv \tag{7}$$

and the total incident power for a plane wave source is

$$P_{source}(t) = \int_S |\vec{E}(\vec{r},t)|^2/\eta_0\, ds \tag{8}$$

where $\eta_0 = 377\,\Omega$ is the free space impedance . Since the input source is a modulated sinusoid, direct application of Equation 5 will give the total fraction of light absorbed not the desired fraction absorbed at the center frequency, ω_0. Fourier Analysis is used to calculate the desired $A(\omega_0)$. Specifically, Parseval's Theorem is used to transform the time average integrals to the frequency domain. Parseval's Theorem for a general function, $f(t)$, is

$$\int_{-\infty}^{\infty} f^2(t)\, dt = \frac{1}{2\pi} \int_{-\infty}^{\infty} |F(jw)|^2\, d\omega \tag{9}$$

In words, the power contained in the source, $f(t)$, due to a single harmonic component, ω_0, is $|F(j\omega_0)|^2/2\pi$. $F(j\omega_0)$ is Fourier transform of $f(t)$ evaluated at ω_0. It is a now simple matter to decompose the total absorption into power due to each individual harmonic using Parseval's Theorem to find

$$A(\omega_0) = \frac{\sigma \int_V |\vec{E}(\vec{r},j\omega_0)|^2\, dv}{\int_S |\vec{E}(\vec{r},j\omega_0)|^2/\eta_0\, ds} \tag{10}$$

The time averages are transformed from integrals in the time-domain into a multiplication of the Fourier transformed electric fields in the frequency-domain. $A(\omega_0)$ in Equation 10 is one measure of light-trapping. The maximum achievable current density (MACD) is another measure of light-trapping which takes into account the solar spectrum. The MACD, J_{sc}, is defined by

$$J_{sc} = q \int_0^{\lambda_m} F(\lambda) A(\lambda)\, d\lambda \tag{11}$$

where q is the charge of an electron, $F(\lambda)$ is the solar spectrum (usually AM1.5) of the incident light, and $A(\lambda)$ comes from the solution to Maxwell's equations. Once the absorption spectrum is known (assuming ideal internal spectral response), the MACD is calculated from Equation 11. The ideal internal spectral response makes it possible to study light-trapping without reference to any specific semiconductor material used in the solar cell. In this way, silicon as well as any other semiconductor can be studied based solely on optical considerations.

Both the absorption, $A(\lambda)$, and the MACD are used to quantify light-trapping. In the strict sense, absorption is the pure measure of light-trapping. Absorption quantifies how the incident light is absorbed as a function of wavelength but ignores the spectral content of the sunlight. On the other hand, the MACD integrates the effects of both the absorption and solar spectrum into a single quantity, J_{sc}. The MACD gives a more telling characterization of the real operational solar cell than absorption, without limiting itself to any particular semiconductor.

G. Limitations and Capabilities

The primary limitation of the FDTD model of light-trapping is due to limited computer resources. For example, a modest silicon solar cell which is $1\,\mu$m thick with a periodic boundary has a total volume of $1\,\mu m^3$. The total number of unit cells is 160^3. The total memory requirement is approximately 188 megabytes. Today's standard personal

computer has 16 megabytes of memory, much less than required by the model. The FDTD model falls short of the ray-trace model in this regard.

The FDTD model of light-trapping assumes the geometric features of the solar cell are periodic which reduces computer resource requirements. The solar cell is described by multiple layers of dielectrics. Each dielectric has a complex surface structure, i.e. perpendicular slats, pyramid, tilted-pyramid ...or any surface described by the function, $K(x, y)$. Multiple layer anti-reflection coatings are also included in the model. Modern solar cell designs as thin as $0.5\,\mu$m are potentially very cheap because of their low mass per unit of performance [25]. The combination of the FDTD algorithm, general texture shapes, and anti-reflection coatings enables the solar cell designer to model and design thin solar cells based on light-trapping more accurately than is possible with any ray-trace model.

III. Full Wave Model Light-Trapping Analysis

In this section, the finite-difference time-domain model is applied to the light-trapping analysis of thin silicon solar cells. The thickness of the solar cell is approximately equal to the wavelength of light. The goal of the FDTD model is to accurately predict absorption in thin films. The cost of accuracy is the model's dependence on powerful and expensive computers. Unlike the ray-trace model, the FDTD model is not able to execute on a personal computer with only one megabyte of memory. All the light-trapping analysis presented in this section are executed on Cray supercomputers.

A. Thin Cell

Figure 3 compares the accuracy of the FDTD and ray-trace models. The absorption spectrum is calculated for a thin, $0.75\,\mu$m, planar solar cell. The ray-trace model calculates the average absorption. The FDTD model correctly accounts for the wave nature of light. The FDTD model successfully predicts the maxima and minima. Figure 3 clearly demonstrates the FDTD model is more accurate than the ray-trace model. Note, the analytic solution is not valid for textured solar cells.

B. The Maximum Achievable Current Density and Light-Trapping

The light-trapping capability of a thin silicon solar cell is explored in this subsection. By varying the front and rear surface textures of a $0.75\,\mu$m thick solar cell, the light-trapping capability of some

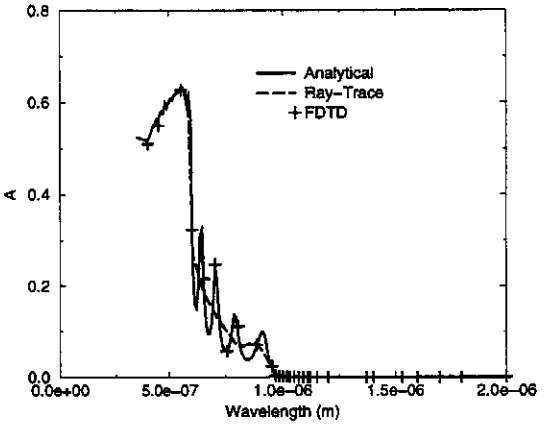

Fig. 3. The absorption of light by a $0.75\,\mu$m untextured solar cell.

promising designs is determined [1], [3], [4], [5], [6], [7], [8], [9]. Figure 4 shows the geometric layout of five solar cells analyzed with the FDTD model. The height of all surface textures is a quarter of the thickness of the cell ($h = t/4$). The peak angle of all surface textures is 70.4°. All the cells are illuminated by AM1.5 sunlight. Each cell in Figure 4 is $0.75\,\mu$m thick. For the planar solar cell, the $0.75\,\mu$m thickness is the distance between the front and rear surface of the silicon slab. For the perpendicular slat solar cell, the definition of thickness is not obvious. Figure 4 has two parallel dotted lines drawn thru each cell. The distance between the two lines is the thickness. The thickness for the perpendicular slat solar cell is not simply the distance between the front and rear surface peaks. Thickness is defined such that different solar cells with equal cross subsectional area, w^2, and equal thickness, t, have equal mass. This definition of thickness ensures a valid comparison between textured and non-textured solar cells always exists. Mass is directly proportional to volume. Thickness is equivalently defined using volume. Two solar cells that are both t microns thick have the same volume per cross subsectional area. For the planar solar cell, the volume of the unit cell is tw^2. The thickness for the planar solar cell is $t = v/w^2$. In general, thickness is defined as $t = v/w^2$. The volume and cross subsectional area are the same for each of the cells in Figure 4. The ratio between volume and cross subsectional area remains constant such that $t = v/w^2 = 0.75\,\mu$m. Figure 5 summarizes the results of the FDTD light-trapping analysis. All of the textured $0.75\,\mu$m solar cells increase the absorp-

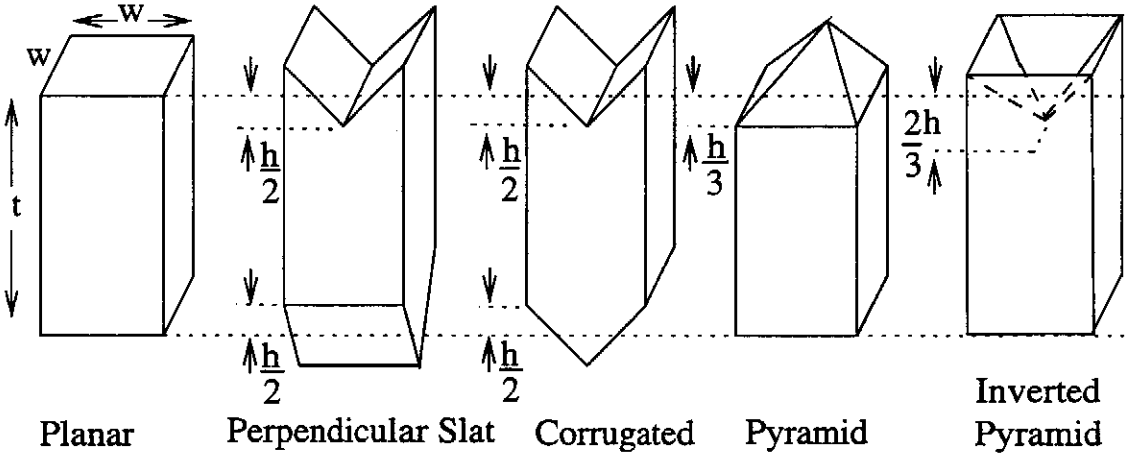

Fig. 4. The thin solar cells analyzed with the FDTD model ($t = 0.75\,\mu$m $h = t/4$ and $\theta = 70.4°$).

TABLE I
THE MACD OF DIFFERENT $0.75\,\mu$M THICK SOLAR CELL DESIGNS.

Design	MACD (mA/cm^2)
Planar	10.4
Corrugated	15.8
Inverted Pyramids	16.9
Perpendicular Slats	17.3
Pyramids	18.1

tion compared to the planar solar cell. The corrugated slat and the inverted pyramid designs do not perform as well as the perpendicular slat design. The perpendicular slat and pyramid designs achieve at least 50% more absorption than the planar solar cell at the shorter wavelengths. The maximum achievable current density (MACD) under AM1.5 illumination for each of the $0.75\,\mu$m designs is tabulated in Table I. The perpendicular slat design has a MACD which is 66% greater than the planar solar cell. The ray-trace model predicts a 12% improvement when the perpendicular slat and planar solar cells are $50\,\mu$m thick. The effect of texturing is more important as the solar cells thickness decreases. The solar cell with the front pyramid surface texture has the highest MACD of $18.1\,mA/cm^2$. This is contrary to the ray-trace prediction that the perpendicular slat solar cell has the higher MACD.

C. Where are the Photons Absorbed?

The ray-trace model [11] shows that the MACD is not the best figure of merit for light-trapping. Based solely on the MACD and the ray-trace model, the best light-trapping design is a thick solar cell with a front surface texture. The MACD makes the false assumption that every absorbed photon contributes to the net current of a solar cell. On the contrary, the net current depends on where the photons are absorbed and the quality of the semiconductor.

What is the generation rate for a thin textured solar cell? The generation rate, $G(\vec{r},\omega)$, must satisfy

$$F(\omega)A(\omega) = \int_V G(\vec{r},\omega)\,dv \qquad (12)$$

where $F(\omega)$ is the solar spectrum and the total absorption, $A(\omega)$, is given by Equation 10. Substitution of Equation 10 into Equation 12 leads to the generation rate of

$$G(\vec{r},\omega) = F(\omega)\frac{\sigma|\vec{E}(\vec{r},j\omega)|^2}{\int_S |\vec{E}(\vec{r},j\omega)|^2/\eta_0\,ds} \qquad (13)$$

In words, the generation rate is directly proportional to the absorption density. From Equation 13 and Equation 10, the absorption density is $G(\vec{r},\omega)/F(\omega)$. The absorption density (the fraction of incident light absorbed per unit volume) is calculated directly by the FDTD model.

Even though it is beyond the scope of this research to use the absorption density to solve the continuity equation, valuable information is gained by looking at the absorption density.

Figure 6 shows the calculated absorption density in the xz- and yz-planes for the planar solar cell. The wavelength of light is $0.35\,\mu$m. The extinction coefficient of silicon at this wavelength is large which

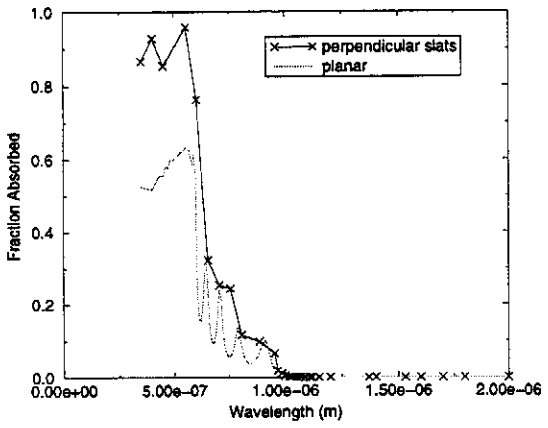

(a) Perpendicular Slats

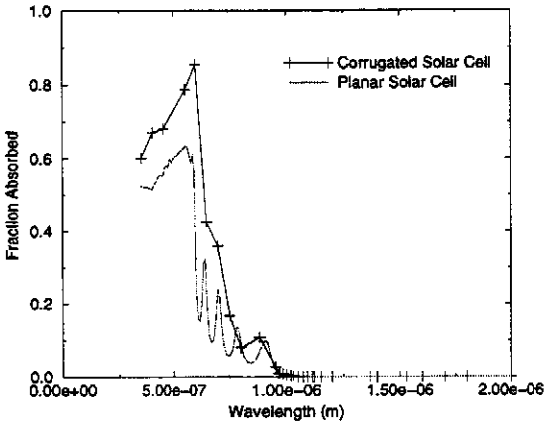

(b) Corrugated Slats

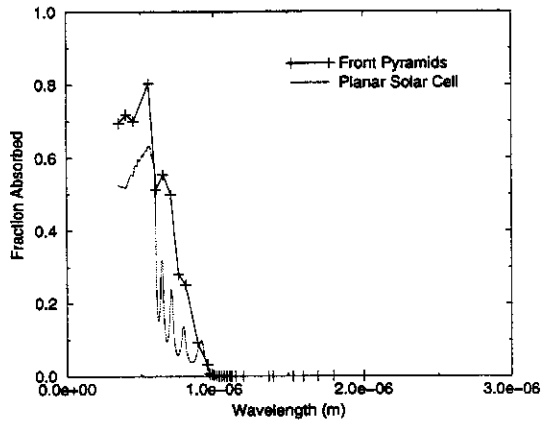

(c) Pyramids

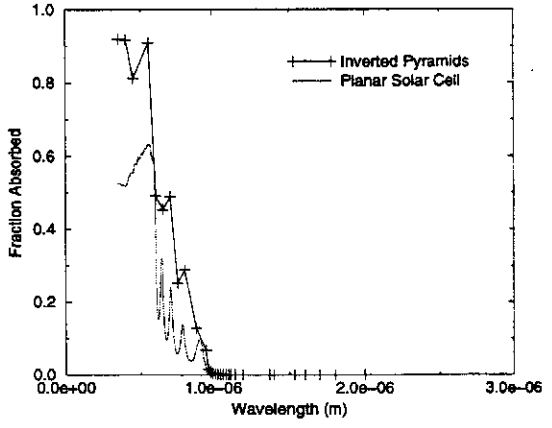

(d) Inverted Pyramids

Fig. 5. The light-trapping capability of different 0.75 μm thick solar cell designs.

leads to the rapid exponential decay of absorption seen in Figure 6. Figure 7 shows the absorption density for the same solar cell except the wavelength of light is 0.70 μm. The low extinction coefficient leads to a uniform average absorption density. The absorption density at the front and rear sides of the solar cell is the same. The FDTD results shows variations in the absorption density caused by the interference of light. Figure 8 illustrates the location of the xz- and yz-planes.

The calculated absorption density for the perpendicular slat solar cell is shown in Figure 9. The wavelength of light is 0.35 μm. Unlike the planar solar cell, the absorption density has an intricate profile. Figure 9 shows most of the light is absorbed near the front surface. The similar effect occurs in the planar cell. Figure 9 shows a sharp peak in the absorption density at the peak of the front surface texture. Figure 10 shows the absorption density for the perpendicular slat solar cell at a wavelength of 0.70 μm. Light reaches the back surface of the solar

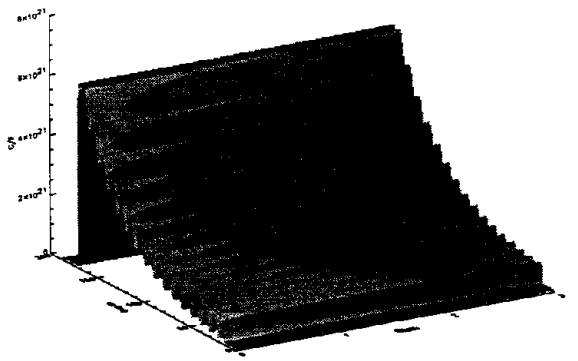

(a) Absorption density in the xz-plane

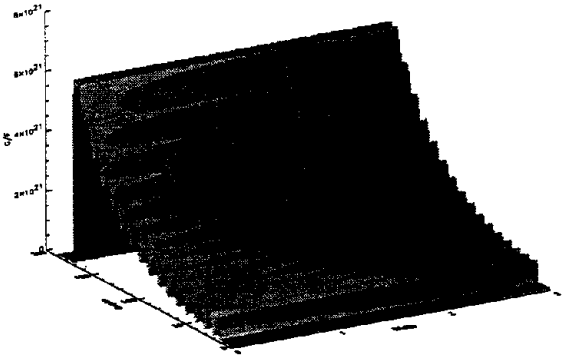

(b) Absorption density in the yz-plane

Fig. 6. The absorption density for the 0.75 μm planar solar cell with $\lambda = 0.35\,\mu$m.

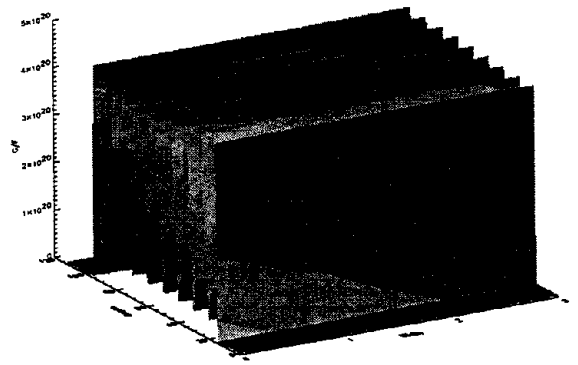

(a) Absorption density in the xz-plane

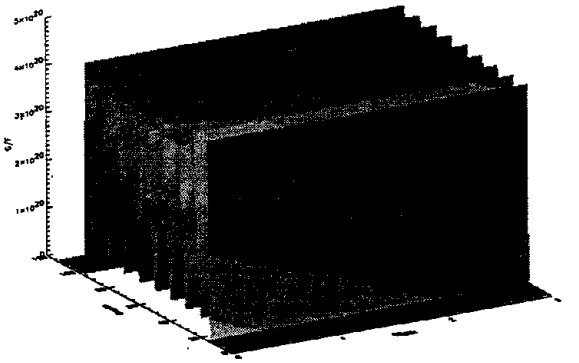

(b) Absorption density in the yz-plane

Fig. 7. The absorption density for the 0.75 μm planar solar cell with $\lambda = 0.70\,\mu$m.

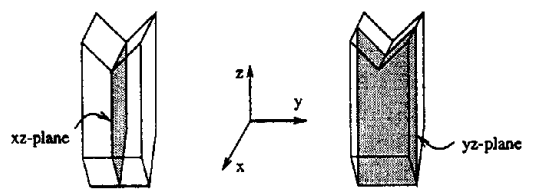

Fig. 8. An illustration of the xz- and yz-planes.

cell. Unexpectedly, the back side of the solar cell has the highest absorption density. The high absorption density at the rear surface is not predicted by the ray-trace model.

D. Summary of Results

The FDTD model is more accurate than the ray-trace model for thin solar cells as shown in Figure 3. Given a solar cell design, the FDTD model calculates the total absorption, the maximum achievable current density, and the absorption density. Based on these output parameters, different solar cell designs are simulated and compared using the FDTD model. The FDTD model indirectly calculates the generation rate. The generation rate is the product of the absorption density and the solar spectrum.

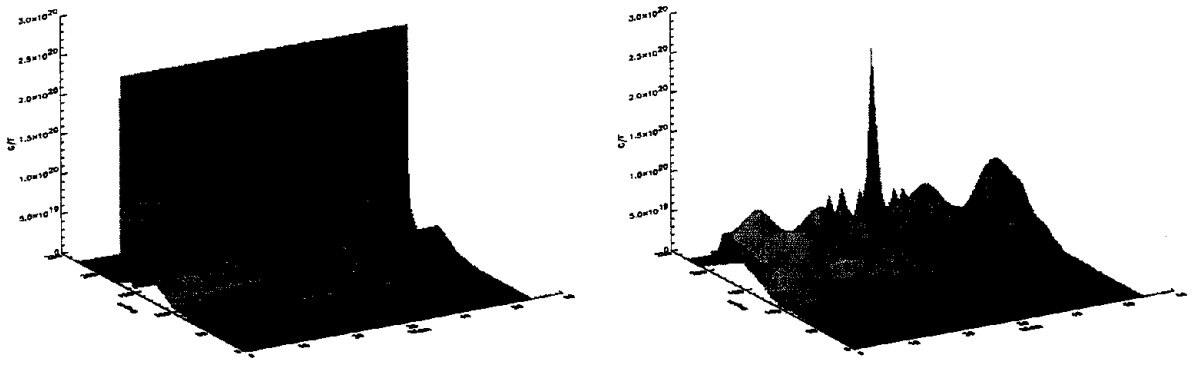

(a) Absorption density in the xz-plane

(b) Absorption density in the yz-plane

Fig. 9. The absorption density for the 0.75 μm perpendicular slat solar cell design with $\lambda = 0.35\,\mu$m.

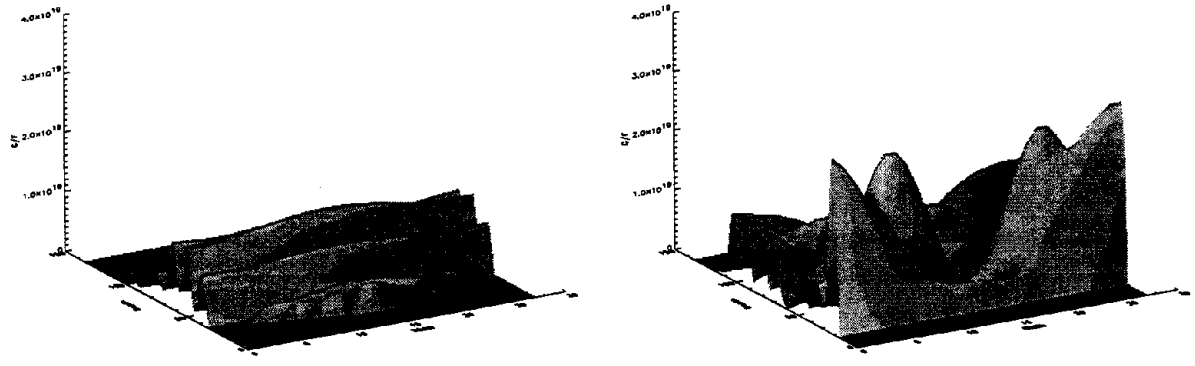

(a) Absorption density in the xz-plane

(b) Absorption density in the yz-plane

Fig. 10. The absorption density for the 0.75 μm perpendicular slat solar cell design with $\lambda = 0.70\,\mu$m.

The generation rate could be used to calculate the expected current density of a solar cell instead of the maximum achievable current density.

Due to the size and complexity of the FDTD model, only a few select solar cell designs are analyzed based on their light-trapping capacity. The MACD for the 0.75 μm thick pyramid solar cell is 18.1 mA/cm^2. The MACD for the 0.75 μm thick perpendicular slat solar cell is 17.3 mA/cm^2. The ray-trace model predicts the perpendicular slat solar cell is better at light trapping than the pyramid design. It is surprising to see the FDTD model predict that the 0.75 μm thick, pyramid design is better. The front pyramid texture increased the MACD by 74% as compared to the planar solar cell. The planar solar cell has a MACD of 10.4 mA/cm^2. For thick solar cells, greater than 50 μm thick, the similar increase in MACD is 12%. Texturing becomes more effective at increasing light-trapping as the thickness of the solar cell decreases.

IV. Discussion

In this research, two computer models have been developed and used to analyze solar cell light-trapping. The characteristic size of the solar cell determines which model is useful. The ray-trace

model is based on the laws of geometrical optics. For this reason, the ray-trace model is limited to thick solar cells [11]. The ray-trace model is inaccurate when applied to the thin 0.75 μm thick planar solar cell. The ray-trace model ignores the wave nature of light and interference effects within the solar cell. The Finite-Difference Time-Domain model is based on solving Maxwell's equations directly. The FDTD model accounts for the wave nature of light. The FDTD model accurately predicts the absorption spectrum for the thin, 0.75 μm, planar solar cell. The FDTD model is applicable to thin solar cells where the characteristic dimension is on the order of the wavelength of light.

The diversity and complexity of possible solar cell designs based on light-trapping creates a large challenge to the engineer. Textured surfaces and anti-reflection films are known to enhance light-trapping. No simple analytical solution to Maxwell's equations exists for the different types of proposed solar cell designs. This problem is relatively easy to overcome by using numerical techniques. Once the numerical model is translated into a computer language, a textured solar cell is as easy to study as a planar solar cell. Neither the ray-trace model nor the FDTD model is limited to planar solar cells. Both models are capable of analyzing the light-trapping characteristics of solar cells with complicated surface textures and anti-reflection films. Both computer models are designed to model complex light-trapping designs. The models also handle dispersive and lossy materials, like silicon.

The solar cells which can be modeled are limited by the available computer resources. The periodic boundary was introduced to partially reduce some of these computer requirements. The ray-trace model was designed to run on an inexpensive personal computer, an Intel-386 based PC with one megabyte of memory. The typical ray-trace analysis of a solar cell requires half a megabyte of memory and about three hours of runtime. However, some runs took as long as a week to analyze a single solar cell. The length of time was dependent on how many rays in the incident beam, the number of textures, and the number of wavelengths. To model dispersion in silicon, a entire run has to be run for each wavelength of incident light. The index of refraction and extinction coefficient are dependent on wavelength. The FDTD model was designed to improve accuracy. One consequence of improved accuracy is the FDTD model cannot run on a personal computer. The biggest limiting factor for the FDTD model is the computer memory requirements. Depending on the wavelength of light, the FDTD analysis of the 0.75 μm thick solar cell required 770 megabytes at the wavelength of 0.35 μm. This large memory requirement is due to the large index of refraction (5.442) for silicon. At the highest wavelength of 2 μm, the memory requirement is only 20 megabytes.

A planar solar cell 0.75 μm thick has a maximum achievable current density of 10 mA/cm^2. The MACD is increased by 74% to 18.1 mA/cm^2 by texturing the front surface of the solar cell with pyramids. The perpendicular slat solar cell configuration increased the MACD by only 66%. The absorption density in the thin solar cell is more complicated than the standard exponential decay seen in thick planar solar cells. The absorption density in a textured solar cell can be larger at the back surface than at the front surface. Surface recombination may be most important at the back side of a thin solar cell. Overall, the FDTD model demonstrates texturing has a large effect on light-trapping in thin solar cells.

A. Topics for Future Research

There are several areas of light-trapping which are of interest to the solar cell community and require further investigation. FDTD analysis was verified for planar solar cells, however, the surprising result of the perpendicular slat solar cell FDTD analysis necessitates that experimental verification be done to confirm the modeling technique for textured surfaces. Future investigation could also include improving the FDTD model to analyzing new light-trapping designs. The ability to accurately model thin solar cells brings new avenues to study andenhance light-trapping.

ACKNOWLEDGMENTS

The authors thank Cray Research for supercomputing grants. They also acknowledge the support of Associated Western Universities, Inc. for a Thesis Parts Fellowship. The ray-trace work was supported by the US Department of Energy under contract DOE DE-AC02-83CH10093 and the National Renewable Energy Laboratory under two contracts; CT-2-12285-1 and CAT-4-13527-01.

AUTHORS BIO

Todd Marshall received his BS in Engineering Physics (1993) and his MSEE (1996) from the University of Colorado. He is currently working on his PhD in electromagnetics at the University of Colorado - Boulder.

Melinda Piket-May received her BSEE from the University of Illinois - Champaign (1988) and her MSEE (1990) and PhD (1993) from Northwestern University. She is currently an assistant professor at the University of Colorado - Boulder. She received the URSI Young Scientist Award in 1996 and the NSF CAREER Award in 1997.

REFERENCES

[1] P. Campbell, S.R. Wenham, and M.A. Green, "Light trapping and reflection control in solar cells using tilted crystallographic surface textures," *Solar Energy Materials and Solar Cells*, vol. 31, no. 2, pp. 133–153, November 1993.

[2] Bhushan L. Sopori and Todd Marshall, "Optical confinement in thin silicon films: A comprehensive ray optical theory," in *Conference Record of the Twenty Third IEEE Photovoltaic Specialists Conference*, 1993, pp. 127–132.

[3] T. Tiedje, B. Abeles, J.M. Cebulka, and J. Pelz, "Photoconductivity enhancement by light trapping in rough amorphous silicon," *Applied Physics Letters*, vol. 42, no. 8, pp. 712–714, April 1983.

[4] Martin A. Green, Andrew W. Blakers, Jianua Zhao, Adele M. Milne, Aihua Wang, and Ximing Dai, "Characterization of 23-percent efficient silicon solar cells," *IEEE Trans. on Electron Devices*, vol. 37, no. 2, pp. 331–336, February 1990.

[5] Tsuyoshi Uematsu, Minoru Ida, Kunio Hane, Shigeru Kokunai, and Tadashi Saitoh, "A new cell structure for very thin high-efficiency silicon solar cells," *IEEE Trans. on Electron Devices*, vol. 37, no. 2, pp. 344–347, February 1990.

[6] Patrick Campbell and Martin A. Green, "Light trapping properties of pyramidally textured surfaces," *J. Appl. Phys.*, vol. 62, no. 1, pp. 243–249, July 1987.

[7] H.W. Deckman, C.R. Wronski, H. Witzke, and E. Yablonovitch, "Optically enhanced amorphous silicon solar cells," *Appl. Phys. Lett.*, vol. 42, no. 11, pp. 968–970, June 1983.

[8] Eli Yablonovitch and George D. Cody, "Intensity enhancement in textured optical sheets for solar cells," *IEEE Trans. on Electron Devices*, vol. 29, no. 2, pp. 300–305, February 1982.

[9] B.L. Sopori and R.A. Pryor, "Design of antireflection coatings for textured silicon solar cells," *Solar Cells*, vol. 8, no. 3, pp. 249–261, April 1983.

[10] M. A. Green, *Chapter 15: Surface Texturing and Patterning in Solar Cells*, pp. 231– 269, American Solar Energy Society, 1993.

[11] T. Marshall and M. Piket-May, "Numerical model of light-trapping in solar cells," *Applied Computational Electromagnetics Society Journal*, Submitted January 1997.

[12] K.S. Yee, "Numerical solution of initial boundary value problems involving maxwell's equations in isotropic media," *IEEE Trans. on Antennas and Propagat.*, vol. 14, pp. 302–307, 1966.

[13] Allen Taflove, *Computational Electrodynamics the Finite-Difference Time-Domain Method*, pp. 98–100,111–134,281–295, Artech House, Boston, 1995.

[14] A. Taflove and M.E. Brodwin, "Numerical solution of steady-state electromagnetic scattering problems using the time-dependent maxwell's equations," *IEEE Trans. on Microwave Theory Tech.*, vol. 23, pp. 623–630, 1975.

[15] F.L. Pedrotti and L.S. Pedrotti, *Introduction to Optics*, pp. 42,466,485–487, Prentice-Hall, Englewood Cliffs, New Jersy, 1987.

[16] E.D. Palik, Ed., *Handbook of Optical Constants of Solids*, p. 547, Academic Press, 1985.

[17] A. Bayliss and E. Turkel, "Radiation boundary conditions for wave-like equations," *Comm. Pure Appl. Math*, vol. 23, pp. 707–725, 1980.

[18] B. Engquist and A. Majda, "Absorbing boundary conditions for the numerical simulation of waves," *Mathematics of Computation*, vol. 31, pp. 629–651, 1977.

[19] L.N. Trefethen and L. Halpern, "Well-posedness of one-way wave equations and absorbing boundary conditions," *Mathematics of Computation*, vol. 47, pp. 421–435, 1986.

[20] G. Mur, "Absorbing boundary conditions for the finite-difference approximation of the time-domain electromagnetic field equations," *IEEE Trans. on Electromagnetic Compatibility*, vol. 23, pp. 377–382, 1981.

[21] R.L. Higdon, "Numerical absorbing boundary conditions for the wave equation," *Mathematics of Computation*, vol. 49, pp. 65–90, 1987.

[22] K.K. Mei and J. Fang, "Superabsorption-a method to improve absorbing boundary conditions," *IEEE Trans. on Antennas and Propagat.*, vol. 40, pp. 1001–1010, 1992.

[23] J.P. Berenger, "A perfectly matched layer for the absorption of electromagnetic waves," *Journal of Computational Physics*, vol. 114, pp. 185–200, 1994.

[24] D.S. Katz, E.T. Thiele, and A. Taflove, "Validation and extension to three dimensions of the berenger pml absorbing boundary condition for fd-td meshes," *IEEE Microwave and Guided Wave Letters*, vol. 4, pp. 268–270, 1994.

[25] E. Yablonovitch, G.B. Stringfellow, and J.E. Greene, "Growth of photovoltaic semiconductors," *Journal of Electronic Materials*, vol. 22, no. 1, pp. 49–55, 1993.